

SIMULATION OF VESTIBULAR IMPLANT STIMULATION IN HUMAN INNER EAR ANATOMY WITH REGISTERED SYNTHETIC COCHLEA STRUCTURE

M. Handler¹, S. D'Alessandro¹, R. Saba², D. Baumgarten¹

¹Institute of Electrical and Biomedical Engineering, UMIT - Private University for Health Sciences, Medical Informatics and Technology, Hall in Tirol, Austria

²MED-EL GmbH, Innsbruck, Austria

michael.handler@umit-tirol.at

Abstract— A human inner ear model was extended to include a synthetic cochlea model for analyzing unintended stimulation of the auditory nerve by a vestibular implant. Stimulation amplitudes for activation of the auditory nerve during monopolar vestibular stimulation were simulated as well as alterations in neural activation of other nerve branches due to the insertion of the synthetic cochlea. Only small deviations were found for stimulus amplitudes and neural activation in neighboring nerve branches, indicating a negligible effect on the overall stimulation result when including the synthetic cochlea model. A more complete picture of the stimulation outcome can be obtained by considering the synthetic cochlea instead of incomplete segmentations of the auditory nerve.

Keywords— Vestibular implant, virtual model, synthetic cochlea, human anatomy, nerve stimulation

Introduction

Vestibular implants offer a potential treatment option for patients suffering from bilateral vestibular dysfunction to improve their sense of balance and spatial orientation. Human clinical studies and experimental evaluations considering animal models have been performed focusing on the improvement of vestibular implants and applied stimulation scenarios (e.g., [1]). In addition, also computer models have been used to analyze the effects of vestibular stimulation scenarios taking into account realistic inner ear anatomies of animals [2, 3] as well as human inner ear anatomies based on simplified synthetic models [4]. In our studies computer models based on μ CT-scans of excised human specimen have been used to optimize selective vestibular nerve stimulation and minimize stimulation of nearby non-targeted nerves [5, 6]. For the evaluation of selective nerve stimulation and for considering anisotropic electrical properties in the computer models, 400 neurons were defined for each nerve branch in the models by paths starting from the most peripheral regions of the nerves and growing towards the central part of the inner auditory canal (IAC). For a detailed description of the nerve fiber generation algorithm, the reader is referred to [5, 6]. Neurons of the auditory nerve could not be considered in these computer simulations, because the domain of the auditory nerve could not be properly labeled due to insufficient spatial resolution and in-

complete uptake of staining agent. However, the consideration of cochlear neurons in the simulations would allow for evaluating possible unintended stimulation of the auditory nerve caused by current spreads of a vestibular implant – a potential limiting factor for the selection of electrode and stimulation configurations.

In this work, a synthetic cochlear model was integrated in an existing human inner ear model to allow for the analysis of unintended stimulation of the auditory nerve by vestibular implants. A workflow is described for model preparation, replacement of the incompletely labeled cochlea by the synthetic model and nerve fiber generation. Finally, resulting nerve fiber activations after stimulation by monopolar electrode configurations are evaluated and compared between models with the originally labeled incomplete cochlea and the extended model.

Methods

The human inner ear model used in this study is based on a μ CT-scan of a vestibular specimen of a donated body of a 78-year-old male. This model corresponds to Model 3 in [5]. For further details regarding the specimen preparation and segmentation, the reader is referred to our previous work [5]. Fig. 1 depicts the inner ear model focusing on the segmented structure of the auditory nerve. Due to the disconnected regions in the segmentation, nerve fibers could not be generated by our previously described algorithm [5] for this and similar models.

A CAD-model of a human auditory nerve and the combined scala tympani, scala vestibuli and scala media was created based on a human inner ear model. This model was used as synthetic cochlea to replace the incomplete structure of the originally labeled auditory nerve and cochlear scalas. In an initial registration step, a landmark-based registration approach was performed. Surface models of both the originally segmented auditory nerve and combined cochlear scalas were created. The surface models of the CAD geometry of the auditory nerve were registered to the originally segmented geometry by a landmark warping approach using ITK [7]. For both the original and synthetic cochlea model, 34 corresponding landmarks were defined manually on the most peripheral sections close to the organ of Corti and along the auditory nerve within the peripheral

section of the IAC as these structures could be identified best in the incomplete segmented data. Additionally, six corresponding landmarks were defined manually on the surfaces of the cochlear scalas for both the original and synthetic cochlear model and a similarity transformation was performed in 3D Slicer [8]. After performing the registration based on manual landmarks, the preliminary result was improved by applying an automatic registration step using the BRAINSFit library [9] in 3D Slicer [8]. The result of the registration of the auditory nerve of the synthetic CAD model to the originally labeled auditory nerve is shown in Fig. 2.

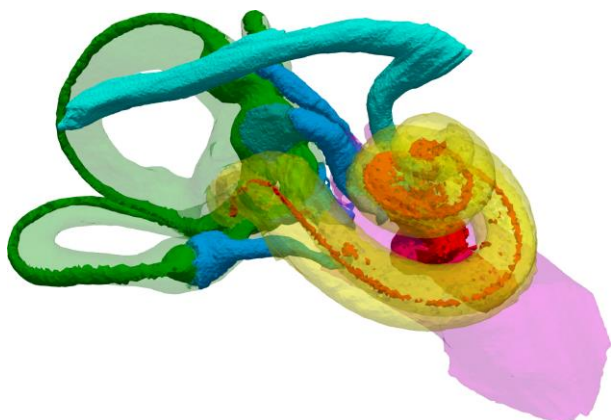


Figure 1: Human inner ear model with incompletely segmented auditory nerve, making the generation of an anisotropy field and virtual nerve fibers for the auditory nerve impossible for the algorithms described in our previous work [5].

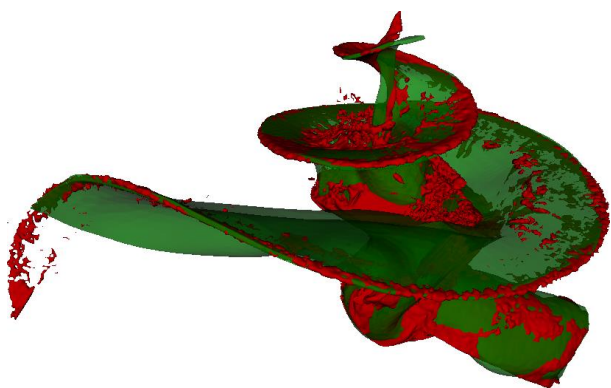


Figure 2: Original segmentation of auditory nerve (red) superimposed by the registered CAD model of the auditory nerve (green).

Next, the original segmentation result was smoothed to improve the quality of the meshing result in a later step. The segmented cochlea, all vestibular nerves and the facial nerve were removed from the model by replacing the corresponding labels in the segmentation by the label of the closest surrounding voxel. The registered cochlea was then inserted into the model by replacing the labels of the corresponding voxels by the registration result. After the insertion of the synthetic cochlea, the previously removed vestibular nerves and the facial nerve were also inserted again

into the model. These additional steps for the vestibular nerves and the facial nerve were necessary to preserve their shapes in the model as the removal of the cochlea causes all neighboring structures to grow into the regions previously occupied by the original cochlea.

Two tetrahedra meshes were created for the original model with incomplete auditory nerve and the model considering the synthetic cochlea. The segmented components were surrounded by a spherical bone domain (diameter 5 cm) with low electric conductivity representing the temporal bone in the model, and the bone sphere was surrounded by a conductive layer of 1 cm thickness, similar to the work described in [4]. The model creation workflow is described in more detail in our previous work [5, 6]. Vector fields defining the fiber orientation for all nerves were created as explained in this previously described model creation workflow to consider anisotropic electrical conductivity tensors in the finite element model and to generate virtual nerve fibers for the evaluation of neural activation. For the auditory nerve of the model including the synthetic cochlea, a surface close to the organ of Corti was defined as the starting surface for the virtual nerve fibers, which grow from this starting surface towards the IAC.

Spherically shaped electrode contacts with a diameter of 300 μm were inserted in the ampullae of the anterior, lateral and posterior semicircular canals (SCCs) in both models to test for differences in the stimulation outcome between the models and for unintended neural activation of the auditory nerve caused by electrical stimulation of a vestibular implant. A biphasic stimulus current waveform (a 200 μs cathodic phase followed by a 200 μs anodic phase separated by a 30 μs interphase gap) was applied for each electrode contact separately at increasing amplitudes to evaluate active percentages of the different nerve branches in the model. The reference voltage and current sink electrode contact was considered at the outer boundary of the model. Fig. 3 depicts the model considering the registered synthetic cochlea, nerve fibers and electrode contacts in the ampullae.

Results

Fig. 4 shows the voltage distribution for the model considering the synthetic cochlea when applying a unit current (1 mA) via the electrode contact within the ampulla of the anterior SCC together with the voltage difference relative to the original model with incomplete auditory nerve. While the voltage distribution in the vestibular system is nearly unaffected by the insertion of the synthetic cochlea, slightly higher potentials are found at the auditory nerve and the IAC.

Fig. 5 depicts the fiber activation for every nerve branch in both models during stimulation by the electrode contact in the ampulla of the anterior SCC. First fibers of the auditory nerve (Cochlea) are activated

only at higher stimulus amplitudes of approximately 900 μA with an almost linear increase of activated fibers up to 3 mA, where more than 40 % of the nerve fibers of the cochlea are activated. A similar activation profile for the auditory nerve was also simulated when stimulating with the electrode contacts in the ampullae of the lateral and posterior SCCs (not shown). Only minimal differences in the nerve fiber activation profiles were found for the other nerve branches when comparing the original model with the model considering the synthetic cochlea.

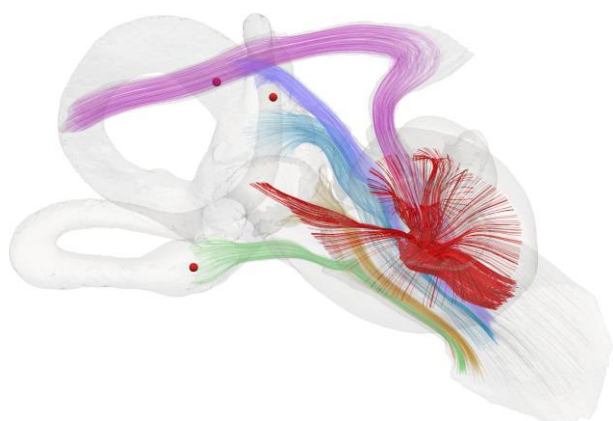


Figure 3: Human inner ear model with generated nerve fibers and inserted electrodes. The registered synthetic cochlea allowed for generating virtual auditory nerve fibers (red lines) for evaluation of unintended stimulation by electrode contacts of a vestibular implant (red spheres).

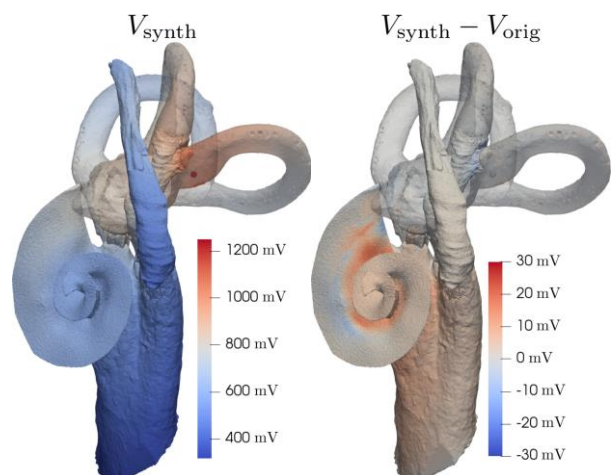


Figure 4: Voltage distribution at applied unit current (1 mA) via the electrode contact in the ampulla of the anterior SCC for the model with synthetic cochlea (V_{synth}) (left) and corresponding voltage difference ($V_{\text{synth}} - V_{\text{orig}}$) compared to the original model with incomplete auditory nerve (V_{orig}) (right).

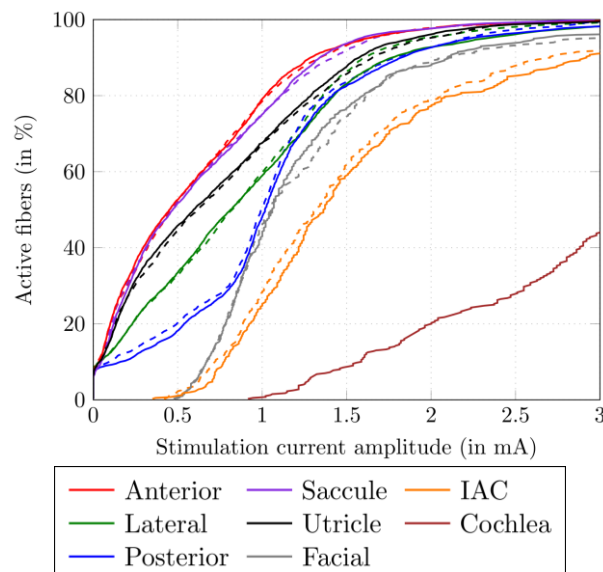


Figure 5: Comparison of neural activation for every nerve branch in the original model with incomplete auditory nerve (dashed lines) and the model with synthetic cochlea (solid lines) during stimulation by the electrode in the ampulla of the anterior SCC.

Discussion

In this work, previously described models of the inner ear were extended by a synthetic CAD model of the cochlea to allow for additionally evaluating unintended neural activation of the auditory nerve during targeted stimulation of vestibular nerve branches. A particular interest was in analyzing the effects of the replacement of the originally labeled cochlea by the synthetic model on the simulated stimulation outcome, as parts of the model were altered by the replacement procedure and also electrical properties were changed in the domain of the cochlea due to the consideration of anisotropic electrical conductivity for the auditory nerve instead of the previously considered isotropic conductivity.

In the described workflow, a CAD model of the cochlea based on a segmented μCT scan of a human inner ear was considered. To apply this model to specific segmented datasets, the CAD model of the cochlea needs to be deformed to match the shape of the auditory nerve and the combined cochlear scalas. Adapted CAD models of the cochlea are planned to consider significant variations in human cochlear anatomy in datasets we want to use in future simulation studies.

In the current implementation, the activation of the auditory nerve fibers is simulated by the same neural model as that for the vestibular nerve fibers considering adapted fiber diameters (2 μm) and without taking into account synaptic noise and afterhyperpolarization. For a detailed description of the neuron models and considered parameters see [6]. In future simulations it is planned to consider more accurate neural models (e.g., as summarized in [10]) for the auditory nerve to obtain a more reliable stimulation outcome.

The comparison of the voltage distributions during applied unit currents in the analyzed models showed that higher voltages are present in the IAC and the auditory nerve in the model considering the synthetic cochlea. This indicates that stimuli from the vestibular system result in higher voltage amplitudes for the model after the synthetic cochlea was applied, consequently leading to a higher chance of stimulation in these areas.

The resulting nerve fiber activation curves indicate that the stimulation outcome for vestibular nerve branches is not significantly influenced by replacing the incomplete cochlea model in the datasets by the registered CAD model of the cochlea. The small deviations in the results of the models depicted in Fig. 5 are mainly caused by differences in nerve fiber distributions within the corresponding nerve branches. On the one hand, these alterations in nerve fiber pathways derive from altered mesh resolutions caused by the replacement of the original cochlea by the synthetic cochlea. On the other hand, also different random seed distributions in both models for the nerve fiber generation slightly influence the computed nerve fiber pathways.

Additional analysis of unintended stimulation of auditory nerve fibers is possible by considering the synthetic cochlea in the human inner ear model during simulation of vestibular implant stimulation scenarios. In a next step it is planned to take into account anatomically more accurate surroundings of the inner ear in the simulations. Realistic human head models would allow for considering realistic reference electrode positions (e.g., below the scalp behind the auricle) and regions with heterogeneous electrical properties between stimulation and reference electrode contacts. Consequently, more realistic voltage distributions and stimulation outcomes can be simulated, leading to an improved reliability of answers to scientific questions provided by the performed in-silico experiments.

Acknowledgements

The authors wish to thank individuals who donated their bodies and tissues for the advancement of education and research. The authors would like to thank the Medical University of Innsbruck for providing labelled high-resolution μ CT-scans of human vestibular anatomy. This work was supported by the federal state of Tyrol within the K-Regio program (project eVITA). This project is co-funded by the European Fund for Regional Development (EFRE).

References

[1] Cr tallaz, C., Boutabla, A. et al.: Influence of systematic variations of the stimulation profile on responses evoked with a vestibular implant prototype in humans, *J. Neural Eng.*, vol. 17, pp. 036027, 2020

- [2] Hayden, R., Sawyer, S. et al.: Virtual labyrinth model of vestibular afferent excitation via implanted electrodes: validation and application to design of a multichannel vestibular prosthesis, *Exp Brain Res*, vol. 210, pp. 623–640, 2011
- [3] Hedjoudje, A., Hayden, R. et al.: Virtual Rhesus Labyrinth Model Predicts Responses to Electrical Stimulation Delivered by a Vestibular Prosthesis, *JARO*, vol. 20, pp. 313–339, 2019
- [4] Marianelli, P., Capogrosso, M. et al.: A Computational Framework for Electrical Stimulation of Vestibular Nerve, *IEEE Transactions on Neural Systems and Rehabilitation Engineering*, vol. 23, pp. 897–909, 2015
- [5] Handler, M., Schier, P.P. et al.: Model-Based Vestibular Afferent Stimulation: Modular Workflow for Analyzing Stimulation Scenarios in Patient Specific and Statistical Vestibular Anatomy, *Front. Neurosci.*, vol. 11, pp. 713, 2017
- [6] Schier, P.P., Handler, M. et al.: Model-Based Vestibular Afferent Stimulation: Evaluating Selective Electrode Locations and Stimulation Waveform Shapes, *Front. Neurosci.*, vol. 12, pp. 588, 2018
- [7] McCormick, M.M., Liu, X. et al.: ITK: enabling reproducible research and open science, *Front. Neuroinform.*, vol 8, pp. 13, 2014
- [8] Fedorov, A., Beichel, R. et al.: 3D Slicer as an Image Computing Platform for the Quantitative Imaging Network, *Magn Reson Imaging*, vol. 30, pp. 1323–1341, 2012
- [9] Johnson, H., Harris, G., and Williams, K.: BRAINSFit: mutual information rigid registrations of whole-brain 3D images, using the insight toolkit, *The Insight Journal*, vol. 57, 2007
- [10] Bachmaier, R., Encke, J. et al.: Comparison of Multi-Compartment Cable Models of Human Auditory Nerve Fibers, *Front. Neurosci.*, vol. 13, pp. 1173, 2019